Thruster Assisted Position Mooring System for Turret-Anchored FPSOs

Asgeir J. Sørensen[1], Jann Peter Strand[2] and Thor I. Fossen[3]

[1]Department of Marine Hydrodynamics/ [3]Department of Engineering Cybernetics, the Norwegian University of Science and Technology, N-7491 Trondheim, Norway.

[2]ABB Industri AS, Marine Division, P. O. Box. 6540, Rodeløkka, N-0501 Oslo, Norway.

E-mail: asgeir.sorensen@marin.ntnu.no, jann-peter.strand@no.abb.com, tif@itk.ntnu.no

Abstract— **A thruster assisted position mooring system includes different control functions for station keeping and motions damping of the horizontal-plane motions. A new nonlinear passivity-based state observer producing the thruster control actions has been implemented and verified in full-scale tests. Even though sophisticated filtering and control techniques are applied in the high-level control systems, unforeseen load peaks caused by process disturbances acting on the local actuation system may challenge the power plant stability, if no proper precaution is taken. Both high and low level control aspects concerning integrated positioning and electrical propulsion system are addressed.**

Keywords— **Marine control systems, positioning, observer**

Fig. 1. Varg FPSO.

I. Introduction

In the North Sea as in several other areas new oil and gas resources are found in smaller or so-called marginal fields. In addition the offshore industry is moving more of the exploration and exploitation activities to fields at deeper water, whereof several of these prospects are located in hostile environments. In this context floating vessels in combination with subsea installations have shown to be the preferred solution.

Use of floating concepts for deep sea drilling, floating production and shuttle tankers have become possible with use of sophisticated control systems for precise and safe positioning. There are two main types of positioning systems: *dynamic positioning (Dynpos) systems* used for positioning of free floating vessels (Sørensen *et al.* [7]) and *thruster assisted position mooring (Posmoor) systems* (Strand *et al.* [10]) used for anchored vessels. Both type of systems may be installed with varying type and number of control functions, sensors and computers with appropriate thruster power capability and configuration depending on safety and availability requirements. This paper will focus on thruster assisted position mooring of turret anchored floating production storage and off-loading (FPSO) ships, see Fig. 2. Conventionally, linear methods are used in the estimation of low-frequency ship motion and non-measured velocities producing the thruster control actions. In order to account for the inherent physical nonlinearities, gain-scheduling techniques are commonly used. This may under certain circumstances result in degraded performance where no global stability can be guaranteed. In this paper the nonlinear passivity-based state observer proposed by Fossen and Strand [4] and Strand and Fossen [9] is implemented in the ABB positioning system. This observer utilize the physical characteristics of the dynamic system in the formulation in order to achieve more robust performance, simplified software algorithms and tuning procedures for commissioning.

The strong requirements to vessel performance, environmental aspects and overall safety have resulted in increased focus on the total vessel concept and the interactions between the different equipment and systems installed. Flexibility in operation has enabled electrical power generation and distribution systems for propulsion, positioning, oil production, drilling, and loading, where all equipment and control systems are integrated into a common power plant network and automation network. In fully integrated systems, functional in addition to physical integration of power, automation and turret systems combined with thorough marine process knowledge introduces new and far better opportunities to optimize the overall vessel mission objective at lower life cycle costs. In order to accomplish this it is essential to properly address the energy control of the consumers and producers of electrical power onboard the vessel. If the various consumers (thrusters, pumps, compressors etc.) of power act separately and uncoordinated from each other, the power generation system must be dimensioned and operated with larger safety margins to account for the corresponding larger mean power demands and unintentionally power peaks. This paper will also illustrate the importance of focusing on low level actuator control, exemplified on thruster control, in order to achieve a thorough successful control result, which does not have negative impact on the other systems on the ship. The

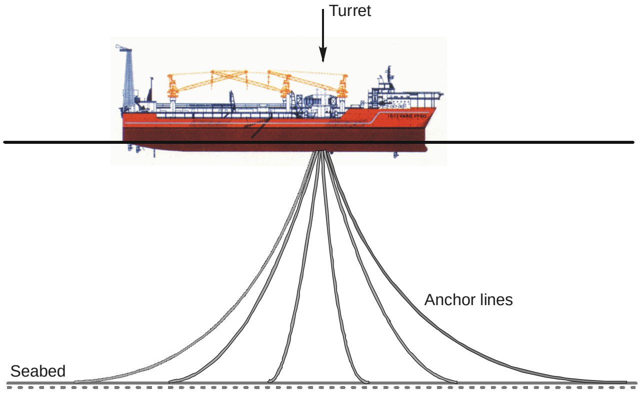

Fig. 2. Turret-anchored FPSO.

performance of the positioning control system is verified by extensive full-scale tests of the Varg FPSO, operated by Saga Petroleum ASA in the North Sea, see Fig. 1.

II. Total Integrated System for FPSOs

A. Integration Aspects

The trend in the market is towards increased system responsibility for vendors of larger packages. In the marine, oil and gas market of power, automation and positioning systems, there is a handful of vendors more or less able to offer total integrated solutions as shown in Fig. 3. The change in methods and design philosophy is driven towards physical and functional integrated solutions due to a mutual interest of the market actors for the following main reasons:

- One contractual partner.
- Reduced risk exposure for customer during construction, commissioning and operation by single system responsibility avoiding sub-optimization, mismatch and divergence in interfacing and functionality.
- Simplified engineering and installation, since functionality and interfaces are built in well proven product standards.
- Single point of process signal interface and use of fieldbus process I/O give reduced cabling, installation and commissioning costs.
- Reduced maintenance and extent of spare parts in the unified system.
- Higher system integrity.
- Increased operational availability by focusing on overall vessel mission performance and stability in configuration of control applications rather than sub-optimization of the different sub-systems.
- Improved performance and stability of the power plant by integrating the local control of power drives for the different consumers, such as thruster drives, with high level control systems.
- Safe and ergonomic operation based on uniform man-machine philosophy for all systems.
- Uniform training and documentation.
- Financing support.

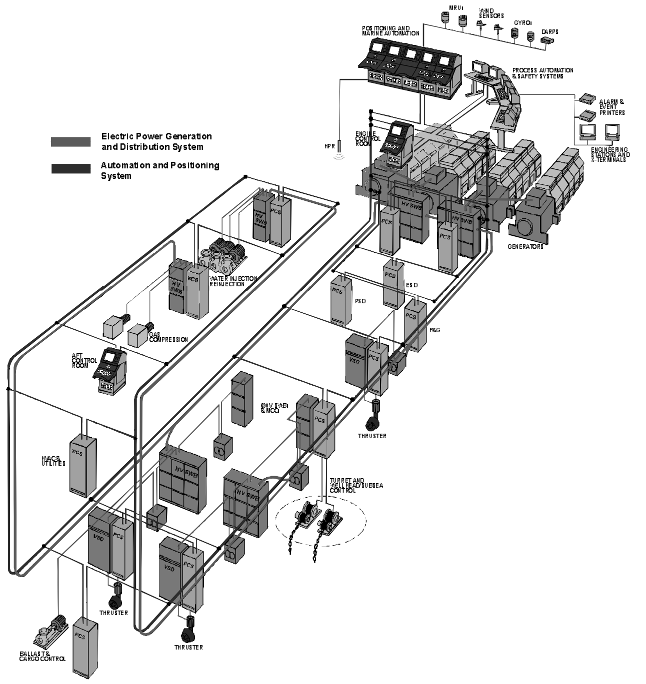

Fig. 3. Ship-based FPSO with total integrated power, automation, positioning, propulsion and turret system.

B. Power Plant

The power generation and distribution system is divided into the following main parts:

- Power plant with prime mover and generator.
- Medium voltage switchboards and bus tie breakers or bus transfers for cross feeding between switchboards.
- Voltage conditioners or filters for reducing harmonic interference.
- Transformers for feeding of alternate voltage levels.
- Low voltage switchboards and motor control centers.
- Rotating converters for frequency conversion and clean power supply.
- Uninterruptible power supply of sensitive equipment and automation systems.

C. Automation System

The merging of software and hardware platforms in automation systems has enabled totally integrated automation system comprising:

- Dynpos control system/Posmoor control system.
- Energy/power management system.
- Vessel automation and HVAC control systems.
- Cargo and ballast control.
- Process automation system.
- Emergency shutdown and fire and gas detection systems.
- Off-loading control system.

D. Posmoor Control System

The Posmoor control architecture consists of the modules illustrated in Fig.4. In position mooring the thruster assistance is complementary to the mooring system. Normally, most of the station keeping in surge and sway will

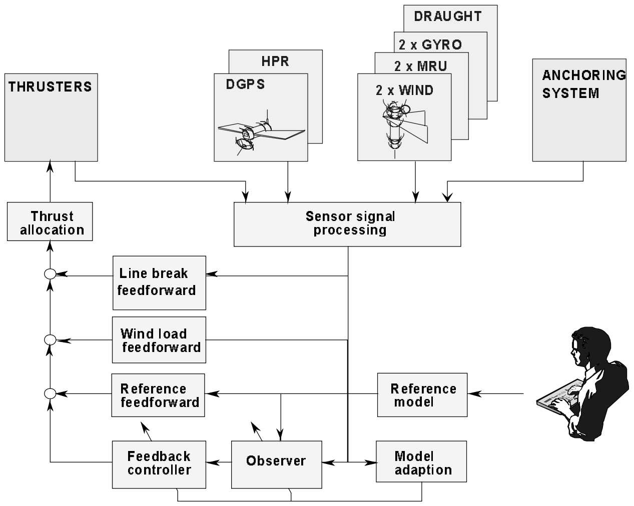

Fig. 4. Posmoor controller architecture.

be provided by the mooring system. The Posmoor control functionality is closely connected to the surge, sway and yaw degrees of freedom (DOFs), which can be viewed as being independent of the actual thruster configuration:

- **Init Mode** is used for configuration, initialization and supervision of the Posmoor system.
- **Manual Mode**: In this mode all 3 DOFs are controlled manually by a joystick.
- **Semi Auto Mode** is defined as a combination of manual and automatic control of surge, sway and yaw.
- **Auto Mode**:
  – *Damping* control is available in all 3 DOFs in order to reduce possible large oscillatory motions and thus reduce the stress on the mooring system.
  – *Station Keeping* operation is to keep the vessel at a fixed position and heading.
  – *Marked Position* represents tracking control in all 3 DOFs, where the vessel moves from the existing position and heading towards new position and heading set-points specified by the operator.
  – *Weather Optimal Positioning* provides continuously updates of the heading such that the environmental loads acting on the vessel are minimized, thereby minimizing the thruster energy consumption. Simultaneously, the position is maintained with arbitrary point of rotation defined, see Fossen and Strand [3]. Other optimal criteria accounting for minimum line tension and roll and pitch motions can be incorporated as well.
  – *Roll and Pitch Damping*: For certain marine constructions with small water plane area, such as semi-submersible, undesirable large roll and pitch oscillations may be induced by the thruster actions. Sørensen and Strand [8] has proposed a control strategy for marine vessels, where also roll and pitch motions are accounted for in the positioning controller.

III. MATHEMATICAL MODELING OF TURRET ANCHORED SHIPS

A. Kinematics

The different reference frames used in the paper are described below:

- The Earth-fixed reference frame is denoted as the $X_E Y_E Z_E$-frame with its origin located in the so-called field zero point (FZP).
- The vessel-parallel $X_V Y_V Z_V$-frame is fixed in the Earth-fixed frame and rotated to the desired heading angle ψ_d. The origin is translated to the desired x_d and y_d position coordinates.
- The body-fixed XYZ-frame is fixed to the vessel body with the origin located at the centre of turret (COT) along the centre line and often at the mean oscillatory position in the average water plane with $(x_G, 0, z_G)$.

The horizontal-plane linear and angular velocity of the vessel in the body-fixed frame relative to the Earth-fixed frame is:

$$\dot{\boldsymbol{\eta}} = \mathbf{J}(\psi)\boldsymbol{\nu}. \tag{1}$$

The vectors defining the Earth-fixed vessel position and orientation, and the body-fixed translation and rotation velocities are given by the vectors $\boldsymbol{\eta} = (\mathrm{x}, \mathrm{y}, \psi)^{\mathrm{T}}$ and $\boldsymbol{\nu} = (\mathrm{u}, \mathrm{v}, \mathrm{r})^{\mathrm{T}}$. $\mathbf{J}(\psi)$ is defined as in Fossen [2].

B. Mooring System

Generally, a mooring system consists of n_m lines connected to the structure and horizontally spread out in a certain pattern. The anchor lines are composed of chain, wire lines or synthetic material, often partitioned into several segments of different types and properties. For turret-moored ships, when the turret is rotatable, the relative angle between the turret and the body-fixed frame is given by the *turret angle* α_{tu}. The length of each anchor line is adjusted by winches and determines the pre-tension and thus the stiffness of the mooring system. The anchor lines enter the turret through fairleads below the hull and the coordinates are defined as *terminal points* (TP). Mooring lines are subjected to three types of excitation (Triantafyllou [11]): Large amplitude LF-motions, medium amplitude WF-motions and small amplitude, very high frequency vortex-induced vibrations. For the purpose of Posmoor control system design it is appropriate to consider the mooring lines' influence on the LF-vessel model.

A horizontal-plane spread mooring model can be formulated as:

$$\boldsymbol{\tau}_{\mathrm{mo}} = -\mathbf{J}^{\mathrm{T}}(\psi)\mathbf{g}_{\mathrm{mo}}(\cdot) - \mathbf{d}_{\mathrm{mo}}(\cdot), \tag{2}$$

where $\boldsymbol{\tau}_{\mathrm{mo}} \in \mathbb{R}^3$ is the vector of generalized mooring forces, $\mathbf{d}_{\mathrm{mo}} \in \mathbb{R}^3$ represents the additional damping in the system due to the mooring system, and $\mathbf{g}_{\mathrm{mo}} \in \mathbb{R}^3$ is the Earth-fixed *restoring term*:

$$\mathbf{g}_{\mathrm{mo}} = \sum_{\mathbf{i=1}}^{\mathbf{n_m}} \begin{bmatrix} H_i \cos\beta_i \\ H_i \sin\beta_i \\ H_i \bar{x}_i \sin\beta_i - H_i \bar{y}_i \cos\beta_i \end{bmatrix}, \tag{3}$$

which is the vectorial sum of the force contribution from each line. H_i is the horizontal force at the attachment point of the ship along the direction of line i, and β_i is the earth-fixed direction of the line. $\bar{x}_i$ and $\bar{y}_i$ are the corresponding moment arms. In a *quasi-static* approach, by disregarding the dynamic effects in the mooring lines, the restoring forces $\mathbf{g}_{\rm mo}$ are treated as function of the low-frequency ship position and heading $\boldsymbol{\eta}$ only according to:

$$\mathbf{g}_{\rm mo} \overset{\rm q.s.}{\approx} \bar{\mathbf{g}}_{\rm mo}(\boldsymbol{\eta};\alpha_{\rm tu}), \tag{4}$$

where the horizontal force contributions H_i in (3) are replaced by the *static line characteristics* (distance/force relationships) for each line i by:

$$\bar{H}_i = f_{Hi}(h_i), \tag{5}$$

which is a function of the horizontal distance h_i between TP and the anchor of each line. About a working point the line characteristics (5) can be linearized by:

$$\bar{H}_i = \bar{H}_{oi} + \left.\frac{df_{Hi}}{dh_i}\right|_{h_i=h_{io}} \Delta h_i, \tag{6}$$

where $\bar{H}_{oi}$ is the average horizontal force in the working point h_{io}, and $\left.\frac{df_{Hi}}{dh_i}\right|_{h_i=h_{io}}$ is the slope of the line characteristics (5) at h_{io}. By assuming fixed anchor line length and neglecting the influence of the current field along the line profile, the generalized mooring forces (2) in a working point can be approximated by a 1st-order Taylor expansion of the static restoring mooring forces and the mooring damping about the working points $\boldsymbol{\eta} = \boldsymbol{\eta}_{\rm o}$ and $\boldsymbol{\nu} = \mathbf{0}$ according to:

$$\begin{aligned} \bar{\mathbf{g}}_{\rm mo}(\boldsymbol{\eta}) &= \bar{\mathbf{g}}_{\rm mo}(\boldsymbol{\eta}_{\rm o}) + \mathbf{G}(\boldsymbol{\eta} - \boldsymbol{\eta}_{\rm o}) + \mathrm{O}(2) & (7) \\ \mathbf{d}_{\rm mo}(\boldsymbol{\nu}) &= \mathbf{D}_{\rm mo}\boldsymbol{\nu} + \mathrm{O}(2), & (8) \end{aligned}$$

where

$$\mathbf{G} = \left.\frac{\partial \bar{\mathbf{g}}_{\rm mo}}{\partial \boldsymbol{\eta}}\right|_{\boldsymbol{\eta}=\boldsymbol{\eta}_{\rm o}}, \quad \mathbf{D}_{\rm mo} = \left.\frac{\partial \mathbf{d}_{\rm mo}}{\partial \boldsymbol{\nu}}\right|_{\boldsymbol{\nu}=\mathbf{0}}. \tag{9}$$

For simplicity, the Earth-fixed frame is often placed in the natural equilibrium point of the mooring system, i.e. $\bar{\mathbf{g}}_{\rm mo}(\boldsymbol{\eta}_{\rm o} = \mathbf{0}) = \mathbf{0}$. Hence, the *quasi-static* mooring model can be written:

$$\boldsymbol{\tau}_{\rm mo} = -\mathbf{J}^{\rm T}(\psi)\mathbf{G}\boldsymbol{\eta} - \mathbf{D}_{\rm mo}\boldsymbol{\nu}. \tag{10}$$

For further details in modelling, see Strand *et al.* [10], Faltinsen [1], Huse and Matsumoto [5] and Triantafyllou and Yue [12].

C. Nonlinear Low-frequency Motion Model

In the mathematical modeling of ship dynamics, it is common to separate the modeling into a low-frequency (LF) model and wave-frequency (WF) model. These two models are assumed to be decoupled. The nonlinear three degrees of freedom body-fixed coupled equations of the LF motion of a marine vehicle in the horizontal-plane can be formulated as:

$$\begin{aligned} &\mathbf{M}\dot{\boldsymbol{\nu}} + \mathbf{C}(\boldsymbol{\nu})\boldsymbol{\nu} + \mathbf{D}_{\rm L}\boldsymbol{\nu} + \mathbf{D}(\boldsymbol{\nu})\boldsymbol{\nu} = \\ &\boldsymbol{\tau}_{\rm thr} + \boldsymbol{\tau}_{\rm mo} + \boldsymbol{\tau}_{\rm wa2} + \boldsymbol{\tau}_{\rm wi} + \boldsymbol{\tau}_{\rm cu}. \end{aligned} \tag{11}$$

The right-hand side of (11) represents generalized external forces acting on the vessel, where $\boldsymbol{\tau}_{\rm thr} \in \mathbb{R}^3$ is the forces and moment generated by the propulsion system, and $\boldsymbol{\tau}_{\rm wa2}, \boldsymbol{\tau}_{\rm wi}, \boldsymbol{\tau}_{\rm cu} \in \mathbb{R}^3$ are the slowly-varying second order wave loads,wind and current loads respectively. $\mathbf{M} \in \mathbb{R}^{3\times3}$ is the inertia matrix including the asymptotic low-frequency hydrodynamic added mass, where the following relation is assumed $\mathbf{M} = \mathbf{M}^{\rm T} > 0$ and $\dot{\mathbf{M}} = \mathbf{0}$. $\mathbf{C}(\boldsymbol{\nu}) \in \mathbb{R}^{3\times3}$ is the skew-symmetric Coriolis and centripetal matrix. $\mathbf{D}_{\rm L} \in \mathbb{R}^{3\times3}$ is the strictly positive linear damping matrix due to laminar skin friction and wave drift damping, and $\mathbf{D}(\boldsymbol{\nu}) \in \mathbb{R}^{3\times3}$ is the nonlinear damping matrix due to viscous effects.

D. Linear Wave-frequency Motion Model

The coupled equations of WF-motions in surge, sway and yaw are assumed to be linear, and can be formulated as:

$$\mathbf{M}(\omega)\ddot{\boldsymbol{\eta}}_{\rm w} + \mathbf{D}_{\rm p}(\omega)\dot{\boldsymbol{\eta}}_{\rm w} = \boldsymbol{\tau}_{\rm wa1}, \tag{12}$$

where the WF-motion vector is defined as $\boldsymbol{\eta}_{\rm w} = (\eta_{\rm w1}, \eta_{\rm w2}, \eta_{\rm w6})^{\rm T}$. $\boldsymbol{\tau}_{\rm wa1} \in \mathbb{R}^3$ is the excitation vector, which will be modified for varying vessel heading relative to the incident wave direction and circular frequency ω. $\mathbf{M}(\omega) \in \mathbb{R}^{3\times3}$ is the mass matrix containing frequency dependent added mass coefficients in addition to the vessel mass and moment of inertia. $\mathbf{D}_{\rm p}(\omega) \in \mathbb{R}^{3\times3}$ is the wave radiation (potential) damping matrix. For simplicity and without loss of generality it is assumed that the mooring system not will influence on the WF-motions.

IV. NONLINEAR PASSIVE OBSERVER DESIGN

A nonlinear observer that can replace the traditional Kalman-filter-based designs has been proposed by Fossen and Strand [4]. This work is further extended by Strand and Fossen [9] to moored ships, where also the dominating WF-motion frequency is adapted.

A. Low-frequency Control Plant Model

For the purpose of model-based controller design it is sufficient to derive a simplified mathematical model, which nevertheless is detailed enough to include the main physical characteristics of the dynamic system. In Posmoor it can be assumed that the vessel velocities are small. Hence, $\mathbf{C}(\boldsymbol{\nu})\boldsymbol{\nu} \approx \mathbf{0}$ and $\boldsymbol{\nu}^{\rm T}\mathbf{D}_{\rm L}\boldsymbol{\nu} \gg \boldsymbol{\nu}^{\rm T}\mathbf{D}(\boldsymbol{\nu})\boldsymbol{\nu}$ can be assumed in (11). In addition by inserting (10) in (11), letting $\mathbf{D}_{\rm L} + \mathbf{D}_{\rm mo} = \mathbf{D} > 0$, and defining a bias term $\mathbf{b} \in \mathbb{R}^3$ accounting for the errors in modeling and external slowly-varying forces and moment due to 2nd-order wave loads, ocean currents and wind, (11) is simplified to:

$$\mathbf{M}\dot{\boldsymbol{\nu}} + \mathbf{D}\boldsymbol{\nu} + \mathbf{J}^{\rm T}(\psi)\mathbf{G}\boldsymbol{\eta} = \boldsymbol{\tau}_{\rm thr} + \mathbf{J}^{\rm T}(\psi)\mathbf{b}. \tag{13}$$

A frequently used bias model for marine control applications is:

$$\dot{\mathbf{b}} = -\mathbf{T}_{\mathrm{b}}^{-1}\mathbf{b} + \mathbf{E}_{\mathrm{b}}\mathbf{w}_{\mathrm{b}}, \tag{14}$$

where $\mathbf{w}_{\mathrm{b}} \in \mathbb{R}^3$ is a zero-mean bounded disturbance vector, $\mathbf{T}_{\mathrm{b}} \in \mathbb{R}^{3\times 3}$ is a diagonal matrix of bias time constants and $\mathbf{E}_{\mathrm{b}}$ a diagonal matrix scaling the amplitude of $\mathbf{w}_{\mathrm{b}}$.

B. *Wave-frequency Control Plant Model*

Based on linear approximations of existing wave spectrum descriptions, see Fossen[2] for details, a linear WF-motion model can be formulated as:

$$\begin{aligned} \dot{\boldsymbol{\xi}} &= \mathbf{A}_{\mathrm{w}}\boldsymbol{\xi} + \mathbf{E}_{\mathrm{w}}\mathbf{w}_{\mathrm{w}} && (15\mathrm{a}) \\ \boldsymbol{\eta}_{\mathrm{w}} &= \mathbf{C}_{\mathrm{w}}\boldsymbol{\xi}, && (15\mathrm{b}) \end{aligned}$$

where $\boldsymbol{\xi} \in \mathbb{R}^{3\cdot \mathrm{p}}$with p as the order of the WF-model, $\mathbf{w}_{\mathrm{w}} \in \mathbb{R}^3$ is a zero-mean bounded disturbance vector and $\mathbf{A}_{\mathrm{w}}$, $\mathbf{C}_{\mathrm{w}}$ and $\mathbf{E}_{\mathrm{w}}$ are constant matrices of appropriate dimensions.

C. *Measurement Model*

Normally, qualified measurements of vessel velocities in the horizontal plane are not available to the positioning system. Hence, the measurement equation is written:

$$\mathbf{y} = \boldsymbol{\eta} + \boldsymbol{\eta}_{\mathrm{w}} + \mathbf{v}_{\mathrm{y}}, \tag{16}$$

which consists of the LF- and WF-motions and measurement noise $\mathbf{v}_{\mathrm{y}} \in \mathbb{R}^3$.

D. *Resulting Control Plant Model*

When designing the observer, the following assumptions are made:

A1 Position and heading sensor noise are omitted, $\mathbf{v}_{\mathrm{y}} = \mathbf{0}$, since this noise is negligeable compared to the wave-induced motion. Especially this is a good approximation for heading measurements, since the gyro compasses are accurate.

A2 The amplitude of the wave-induced yaw motion $\eta_{\mathrm{w}6}$ is assumed to be small, that is less than 1 degree during normal operation of the vessel and less than 5 degrees in extreme weather conditions. Hence, $\mathbf{J}(\psi) \approx \mathbf{J}(\psi + \eta_{\mathrm{w}6})$. From A1 this implies that $\mathbf{J}(\psi) \approx \mathbf{J}(\psi_{\mathrm{y}})$, where $\psi_{\mathrm{y}} \triangleq \psi + \eta_{\mathrm{w}6}$ denotes the measured heading.

Thus, the resulting control plant model can be described by the following equations:

$$\begin{aligned} \dot{\boldsymbol{\xi}} &= \mathbf{A}_{\mathrm{w}}\boldsymbol{\xi} + \mathbf{E}_{\mathrm{w}}\mathbf{w}_{\mathrm{w}} && (17\mathrm{a}) \\ \dot{\boldsymbol{\eta}} &= \mathbf{J}(\psi_{\mathrm{y}})\boldsymbol{\nu} && (17\mathrm{b}) \\ \dot{\mathbf{b}} &= -\mathbf{T}_{\mathrm{b}}^{-1}\mathbf{b} + \mathbf{E}_{\mathrm{b}}\mathbf{w}_{\mathrm{b}} && (17\mathrm{c}) \\ \mathbf{M}\dot{\boldsymbol{\nu}} &= -\mathbf{D}\boldsymbol{\nu} - \mathbf{J}^{\mathrm{T}}(\psi_{\mathrm{y}})(\mathbf{G}\boldsymbol{\eta} - \mathbf{b}) + \boldsymbol{\tau}_{\mathrm{thr}} && (17\mathrm{d}) \\ \mathbf{y} &= \boldsymbol{\eta} + \boldsymbol{\eta}_{\mathrm{w}} = \boldsymbol{\eta} + \mathbf{C}_{\mathrm{w}}\boldsymbol{\xi}. && (17\mathrm{e}) \end{aligned}$$

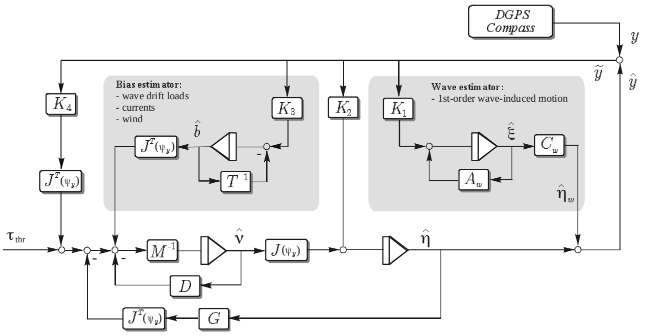

Fig. 5. Block description of the observer.

E. *Observer Equations*

A nonlinear observer is formulated according to:

$$\begin{aligned} \dot{\hat{\boldsymbol{\xi}}} &= \mathbf{A}_{\mathrm{w}}\hat{\boldsymbol{\xi}} + \mathbf{K}_1\tilde{\mathbf{y}} && (18\mathrm{a}) \\ \dot{\hat{\boldsymbol{\eta}}} &= \mathbf{J}(\psi_{\mathrm{y}})\hat{\boldsymbol{\nu}} + \mathbf{K}_2\tilde{\mathbf{y}} && (18\mathrm{b}) \\ \dot{\hat{\mathbf{b}}} &= -\mathbf{T}_{\mathrm{b}}^{-1}\hat{\mathbf{b}} + \mathbf{K}_3\tilde{\mathbf{y}} && (18\mathrm{c}) \\ \mathbf{M}\dot{\hat{\boldsymbol{\nu}}} &= -\mathbf{D}\hat{\boldsymbol{\nu}} + \boldsymbol{\tau}_{\mathrm{thr}} - \mathbf{J}^{\mathrm{T}}(\psi_{\mathrm{y}})(\mathbf{G}\hat{\boldsymbol{\eta}} - \hat{\mathbf{b}} - \mathbf{K}_4\tilde{\mathbf{y}}) && (18\mathrm{d}) \\ \hat{\mathbf{y}} &= \hat{\boldsymbol{\eta}} + \mathbf{C}_{\mathrm{w}}\hat{\boldsymbol{\xi}}, && (18\mathrm{e}) \end{aligned}$$

where $\tilde{\mathbf{y}} = \mathbf{y} - \hat{\mathbf{y}}$ is the innovation vector, and $\mathbf{K}_1 \in \mathbb{R}^{6\times 3}$, and $\mathbf{K}_2, \mathbf{K}_3, \mathbf{K}_4 \in \mathbb{R}^{3\times 3}$ are the observer gain matrices chosen such that the observer becomes passive and GES.

V. RESULTING CONTROLLER

A resulting multivariable control law for station keeping can be formulated as:

$$\boldsymbol{\tau}_{\mathrm{thr}} = -\mathbf{G}_{\nu}\hat{\mathbf{e}}_{\nu} - \mathbf{G}_{\eta}\hat{\mathbf{e}}_{\eta} + \boldsymbol{\tau}_{\mathrm{i}} + \boldsymbol{\tau}_{\mathrm{wff}} + \boldsymbol{\tau}_{\mathrm{lbff}}, \tag{19}$$

where $\hat{\mathbf{e}}_{\nu} = \mathbf{J}^{\mathrm{T}}(\psi_{\mathrm{d}})(\hat{\mathrm{x}} - \mathrm{x}_{\mathrm{d}}, \hat{\mathrm{y}} - \mathrm{y}_{\mathrm{d}}, \hat{\psi} - \psi_{\mathrm{d}})^{\mathrm{T}}$ and $\hat{\mathbf{e}}_{\nu} = (\hat{\mathrm{u}}, \hat{\mathrm{v}}, \hat{\mathrm{r}})^{\mathrm{T}}$. $\boldsymbol{\tau}_{\mathrm{i}}, \boldsymbol{\tau}_{\mathrm{wff}}, \boldsymbol{\tau}_{\mathrm{lbff}} \in \mathbb{R}^3$ are the integral action, the wind feedforward controller and the line break feedforward controller respectively. $\mathbf{G}_{\nu}$, $\mathbf{G}_{\eta} \in \mathbb{R}^{3\times 3}$may be the linear or nonlinear non-negative derivative and proportional controller gain matrices found by appropriate control synthesis methods. One should notice that for the different control functions enabled, different parts of (19) will be activated.

VI. THRUST ALLOCATION

Each thruster unit i will develop a force f_{th}^{i} in a direction α_{th}^{i} such that:

$$\boldsymbol{\tau}_{\mathrm{thr}} = \mathbf{T}_{\mathrm{th}}(\boldsymbol{\alpha}_{\mathrm{th}})\mathbf{f}_{\mathrm{th}} \tag{20}$$

where $\boldsymbol{\alpha}_{\mathrm{th}} \in \mathbb{R}^{\mathrm{m_t}}$ is a vector of thrust directions, $\mathbf{f}_{\mathrm{th}} \in \mathbb{R}^{\mathrm{m_t}}$ is a vector of the developed forces by the thrusters and $\mathbf{T}_{\mathrm{th}}(\boldsymbol{\alpha}_{\mathrm{th}}) \in \mathbb{R}^{3\times \mathrm{m_t}}$ is the thruster configuration matrix. Let the location of each thruster device be denoted $(\mathrm{x}_{\mathrm{th}}^{\mathrm{i}}, \mathrm{y}_{\mathrm{th}}^{\mathrm{i}}, \mathrm{z}_{\mathrm{th}}^{\mathrm{i}})$, relative to the rotation point. Thus, the *i-th* column of $\mathbf{T}_{\mathrm{th}}$ is formulated as:

$$\mathbf{T}_{\mathrm{th}}^{\mathrm{i}} = \begin{bmatrix} \cos\alpha_{\mathrm{th}}^{\mathrm{i}} \\ \sin\alpha_{\mathrm{th}}^{\mathrm{i}} \\ \mathrm{x}_{\mathrm{th}}^{\mathrm{i}}\sin\alpha_{\mathrm{th}}^{\mathrm{i}} - \mathrm{y}_{\mathrm{th}}^{\mathrm{i}}\cos\alpha_{\mathrm{th}}^{\mathrm{i}} \end{bmatrix} \tag{21}$$

The control input to a thruster device, however, are *not* the propeller forces, which cannot be measured directly. Usually the control input $\mathbf{u}_{\mathrm{th}} \in \mathbb{R}^{\mathrm{m}_t}$ is either shaft speed (RPM control) or the pitch ratio of the propeller blades (pitch control), which indirectly controls the developed force according to the so-called *thrust characteristics,* often provided by the propeller vendor:

$$f^i_{\mathrm{th}} = h^i_{\mathrm{th}}(u^i_{\mathrm{th}}), \quad (i = 1, .., m_t) \tag{22}$$

These relations may later be modified during sea trials. However, they are strongly influenced by the local water flow around the propeller blades, hull design, operational philosophy, vessel motion, waves and water current. Defectiveness in these nominal mappings from the actual situation due to local water flow phenomena are not directly compensated for in the overall control system and must be handled by control feedback iterations. A consequence of this is reduced positioning performance with respect to accuracy and response time. In addition, deterioration of performance and stability in the electrical power plant network due to unintentional peaks or power drops caused by load fluctuations on the propeller shafts will occur. Thrusters typically constitute a major part of the total power load. Hence, thruster control approaches that provide more predictable power consumption than the conventional speed and pitch control will subsequently lead to lower total energy consumption. The unpredictable load variations force the operator to maintain a higher level of available power than necessary in order to prevent blackout situations. This implies that the diesel generators will get more running hours at lower loads in average, which in terms gives more wear and tear and maintenance. Sørensen *et al.* [6] suggests using the thruster torque and power consumption as control parameters in order to achieve the desired forces and moment from the thrusters. A total integrated electrical power, automation and positioning system with functional integration will make the method of thrust allocation based on a combination of torque and power control of the propeller and thruster devices into an attractive and feasible solution to overcome these problems. Combination of torque and power control means that the positioning controller's thruster allocation transpose the vessel thrust demand to a torque/power demand instead of a speed reference. This also has to be reflected by certain modifications in the motor control schemes of the electrical motor drive, see Fig. 6.With torque and power control, the propeller load is less sensitive to variations in the surroundings, giving less power disturbances on the network and improved voltage and frequency quality. Additionally, the maximum individual thruster power consumption may easily be limited to the available power in both schemes, since the power limitation is explicit in the torque and power control algorithm. The accurate and fast control of power and power limitation in torque/power control gives less unpredicted load changes, and less need for available power, see Fig. 7.

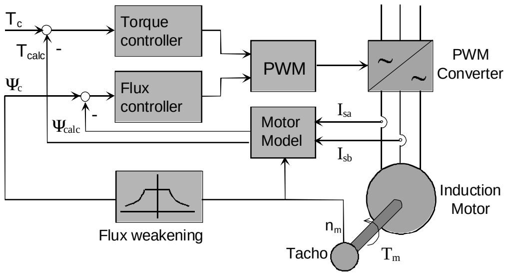

Fig. 6. Simplified block diagram of the torque loop in the electrical motor drive.

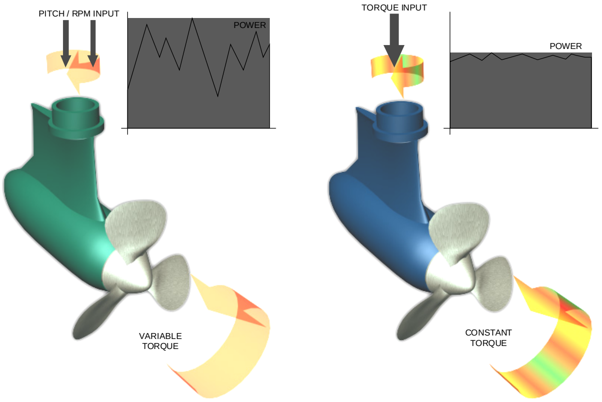

Fig. 7. Torque and power control reduce the dynamic load variations and allows for lower spinning reserves.

VII. Verification Tests on Varg FPSO

In this section results from verification tests of the turret-anchored Varg FPSO, operated by Saga Petroleum ASA at the Varg oil field in the North Sea are presented. In this project ABB has been a total vendor of the integrated automation, power and positioning system. The Posmoor control system is certified according to Posmoor ATA notation, according to the rules of Det norske Veritas Classification [13]. Varg FPSO has length between perpendiculars of 200 meters, ballasted weight of approximately 65000 tons and a weight of 99000 tons in fully loaded condition. The FPSO is equipped with 3 identical azimuth thrusters (variable speed thruster drives), one at the fore and two at the aft, each designed to develop at maximum thrust of approximately 500 kN at 1000 RPM (positive direction). The mooring system consists of 10 anchor lines, spread out in a symmetrical pattern. At the Varg field the water depth is 84 meters. Due to the relatively small water depth, this is a very stiff mooring system with a linear characteristics giving small excursions from the origin, as can be seen in the full-scale results. Two satellite-based positioning systems (DGPS) and one underwater-acoustic-system (HPR) provide measurements of the vessel position. Two gyros measure the vessel heading, two motion reference units measure the roll and pitch orientation and heave motion. Two wind sensors measure the wind speed and direction relative to the ship. Line tension is measured for each mooring line.

The ABB Posmoor control system on Varg FPSO is integrated with the marine and process automation system. It is a redundant system with two operator stations, redundant data busses and two process stations, where the controller is implemented. In addition advisory systems, Posmoor consequence analysis system and Posmoor simulator, are assisting the operator ensuring safe and efficient operation.

A. Log Data

During the tests the FPSO was operating in a weather condition corresponding to: The significant wave height and corresponding dominating wave period was measured by a wave radar to be approximately 6 meters and 10 seconds, respectively. The direction of the waves was approximately +10 deg relative to the bow (attacking starboard). Similarly, the surface current velocity and relative direction was measured to +87 deg and 0.29 m/s. The wind velocity and relative wind direction was measured by the wind sensors and the weighted values are plotted in Figure 11.

During this specific test the Posmoor system was operating with automatic heading control, while surge and sway was manually controlled by the joystick with zero set-points. In Figure 8 the measured position and heading are plotted together with the corresponding LF estimates. The North- East positions are given relative to a pre-defined position on the field (field zero point). Here, the effect of the wave-filtering properties are clearly illustrated. During the time of data acquisition, the azimuth angles were -90 deg for thruster 1 (fore thruster) and $+90$ deg for the aft thrusters (thruster 2 and 3). In Figure 9 the measured RPM is plotted for each of the thrusters.

VIII. Conclusions

In this paper a nonlinear passive observer for thruster assisted position moored ships has been implemented and verified on a full-scale turret-anchored FPSO. Compared to the linear designs, such as the Kalman-filter, the number of tuning parameters was significantly reduced. The observer accounted for the main inherent physical nonlinear characteristics, such as the kinematics. Improved robust performance, simplified software algorithms and tuning procedures for commissioning were achieved. Until recently, the main focus in system integration has been on physical integration of computers and power equipment. However, ABB can by utilizing the benefits of functional integration offer a total integrated solution for anchored marine, oil and gas vessels with improved operational performance and reliability at a minimum of energy consumption and $\mathrm{CO}_x/\mathrm{NO}_x$ emission. Functional integration of power, automation and turret systems combined with thorough marine process knowledge introduced far better opportunities to optimize the overall vessel mission objective. Functional integration has lead to the concept of Energy Management System, with the purpose of optimizing the energy balance in the closed loop energy system on the vessel. Local control of energy consumers was essential in order to have instantaneously control with the present power consumption. The method of thrust allocation based on a combination of torque and power control of the propeller and thruster devices was an attractive and feasible solution to solve these problems, giving less power disturbances on the network and faster and more accurate positioning accuracy.

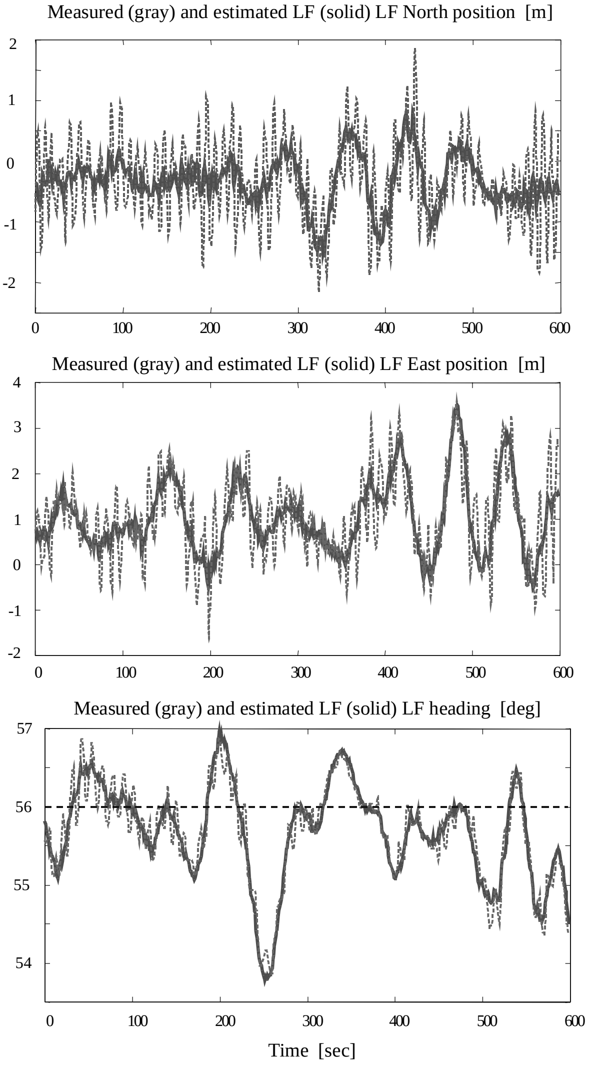

Fig. 8. Measured (dotted) and estimated LF (solid) North and East position (upper and middle) and heading (lower) of Varg.

IX. Acknowledgment

ABB Industri AS and the Norwegian Research Council are gratefully acknowledged for contributions and financial support. Saga Petroleum ASA is gratefully acknowledged for giving permission to publish this paper.

References

[1] Faltinsen, O. M.: 1990, *Sea Loads on Ships and Offshore Structures*. Cambridge University Press.

[2] Fossen, T. I.: 1994, *Guidance and Control of Ocean Vehicles*. John Wiley & Sons Ltd.

[3] Fossen, T. I. and J. P. Strand: 1999a, 'Nonlinear Passive Weather Optimal Positioning Control (WOPC) System for Ships and Rigs: Experimental Results'. Submitted to Automatica.

[4] Fossen, T. I. and J. P. Strand: 1999b, 'Passive Nonlinear Observer Design for Ships Using Lyapunov Methods: Full-Scale Experiments with a Supply Vessel'. *Automatica* **AUT-35**(1), 3–16.

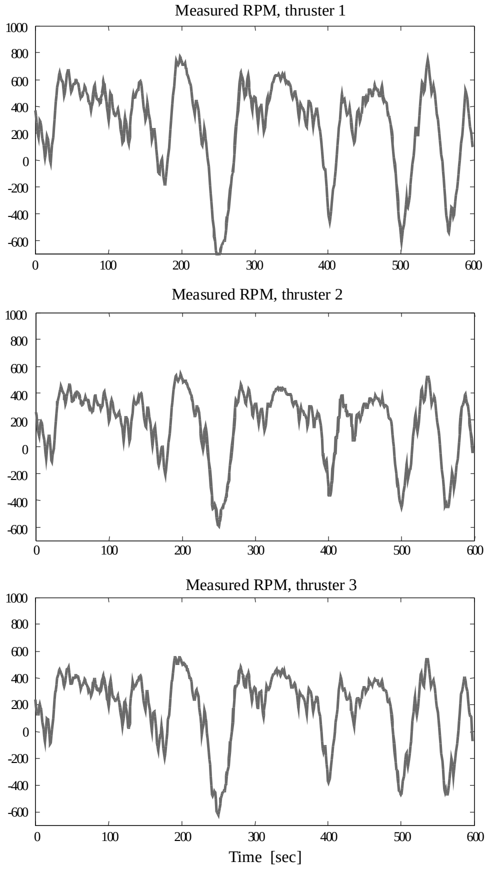

Fig. 9. Thruster action, fore thruster (upper), and aft thrusters (middle and lower) in RPM.

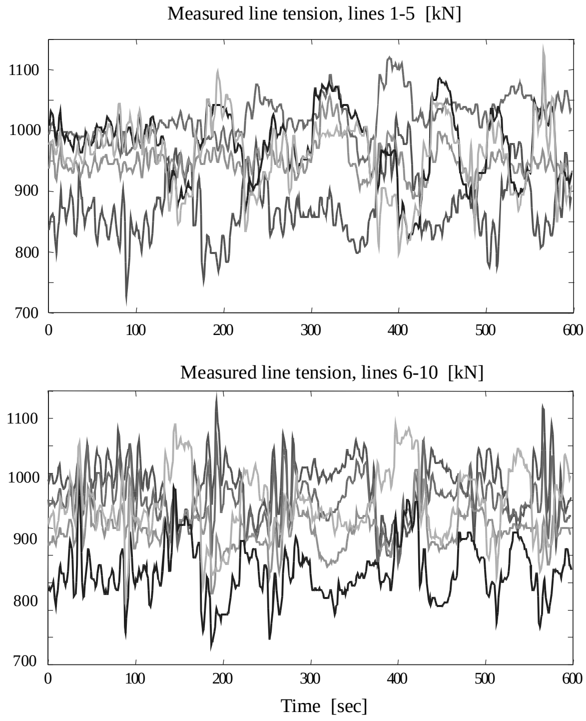

Fig. 10. Measured line tension, lines 1-5 (upper) and lines 6-10 (lower).

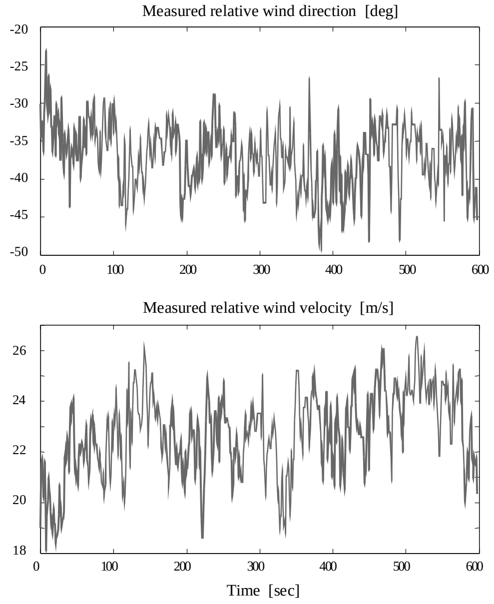

Fig. 11. Measured wind direction (upper) and velocity (lower).

[5] Huse, E. and K. Matsumoto: 1989, 'Mooring Line Damping Due to First- and Second-Order Vessel Motion'. In: *Proc. 21th Annual Offshore Technology Conference.* Houston, Texas, pp. 135–148. Vol. 4, ppr. 6137.

[6] Sørensen, A. J., A. K. Ådnanes, T. I. Fossen, and J. P. Strand: 1997, 'A New Method of Thruster Control in Positioning of Ships Based on Power Control'. In: *Proc. 4th IFAC Conf. On Manoeuvring and Control of Marine Craft (MCMC'97).* Brijuni, Croatia, pp. 172–179.

[7] Sørensen, A. J., S. I. Sagatun, and T. I. Fossen: 1996, 'Design of a Dynamic Positioning System Using Model-Based Control'. *Journal of Control Engineering Practice* **CEP-4**(3), 359–368.

[8] Sørensen, A. J. and J. P. Strand: 1998, 'Positioning of Semi-Submersibles with Roll and Pitch Damping'. In: *Proc. IFAC Conf. On Control Applications In Marine Syststems (CAMS'98).* Fukuoka, Japan, pp. 67–73.

[9] Strand, J. P. and T. I. Fossen: 1999, 'Nonlinear Passive Observer Design for Ships with Adaptive Wave Filtering'. In: H. Nijmeijer and T. I. Fossen (eds.): *New Directions for Nonlinear Observer Design.* Springer Verlag.

[10] Strand, J. P., A. J. Sørensen, and T. I. Fossen: 1998, 'Design of Automatic Thruster Assisted Position Mooring Systems for Ships'. *Modeling, Identification and Control* **MIC-19**(2), 65–71.

[11] Triantafyllou, M. S.: 1994, 'Cable Mechanics for Moored Floating Systems'. In: *BOSS'94.* Boston, MA, pp. 67–77.

[12] Triantafyllou, M. S. and D. K. P. Yue: 1994, 'Damping of Moored Floating Structures'. In: *Proc. 26th Annual Offshore Technology Conference.* Houston, Texas, pp. 215–224. Vol. 3, ppr. 7489.

[13] Veritas: 1996, *Rules for Classification of Mobile Offshore Units, Special Equipment and Systems*, Chapt. Additional Class, Part 6, Chapter 2: Position Mooring (POSMOOR). Det Norske Veritas Classification A/S.